論文内容の要旨

論文題目　Study on CVD Graphene; Doped Impurities and Photoinduced Defects

（化学気相成長グラフェンに関する研究-不純物ドープと光誘起欠陥-）

氏名　今村 岳

1. Introduction

Graphene is a one-atomic thick sheet composed of sp^2 carbon atoms arranged in a honeycomb lattice. Since first isolated in 2004, graphene has been received tremendous attention due to its intriguing properties such as high electron mobility, anomalous quantum Hall effect and long spin coherence length. Doping graphene with heteroatoms, replacing some of carbon atoms in a honeycomb lattice with different atoms, gives rise to some unusual phenomena that cannot be observed in non-doped graphene. It was reported that nitrogen (N)-doped graphene exhibits n-type semiconducting behavior, while pristine graphene shows semi-metallic behavior. It implies doping is a promising method of modifying the electronic structure of graphene, and plays an important role in band gap engineering. Defects and vacancies as well as impurities modify the electronic structure of graphene. Doping heteroatoms to graphene and introducing defects are essential to apply graphene to electronic devices. In this research I develop a method of synthesizing nitrogen-doped graphene and boron (B), N-doped graphene from heteroatom-containing organic molecules and elucidate the relationship between the molecular structures of source materials and the products. I also employ ultraviolet (UV)-irradiation to introduce defects into graphene.

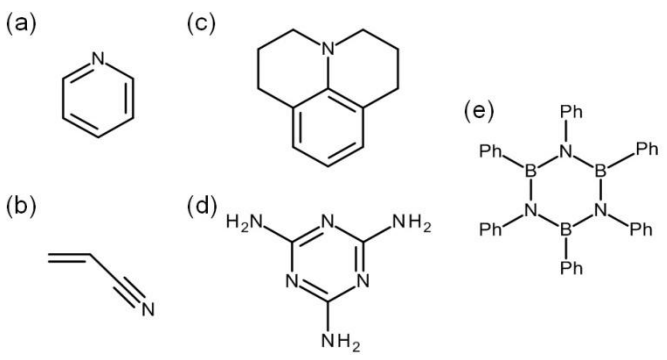

Fig. 1 Molecular structure of (a) pyridine, (b) acrylonitrile, (c) julolidine, (d) melamine, and (e) hexaphenylborazine

2. Synthesis of Doped Graphene from Heteroatom-Containing Organic Compounds

2.1 Synthesis of N-Doped Graphene

N-doped graphene was synthesized on a Pt(111) surface from N-containing molecules via chemical vapor deposition process. Figure 1 shows the four N-containing molecules which were used as source materials of N-doped graphene, pyridine (C_5H_5N), acrylonitrile (C_3H_3N), julolidine ($C_{12}H_{15}N$) and melamine ($C_3H_6N_6$). A Pt(111) surface was cleaned by cycles of Ar^+ sputtering and annealing in an ultrahigh vacuum chamber. The substrate was heated at 500 ℃ and exposed to pyridine, acrylonitrile and julolidine ambient, while melamine was deposited from Knudsen-cell. X-ray photoelectron spectroscopy (XPS) measurements were conducted *in situ* for these samples.

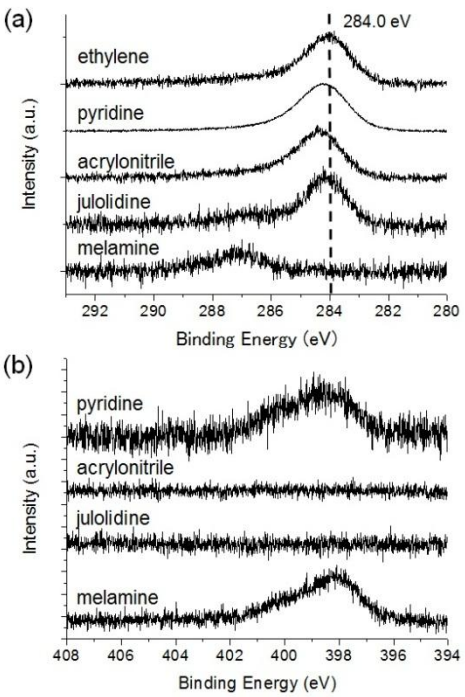

Fig. 2 XPS spectra of the samples in the region of (a) C 1s and (b) N 1s.

Figure 2(a) shows the C 1s region of XPS spectra of the samples. The spectrum of the sample from ethylene is also shown in Fig. 2(a) as a reference since it is already known that graphene is formed from ethylene on a Pt(111) surface. C 1s peaks of the samples indicate graphene was presumably synthesized on a Pt surface from pyridine, acrylonitrile and julolidine because the peaks are positioned at around 284.0 eV, the same peak position as the sample from ethylene (Fig. 2(a)). In a region of N 1s (Fig. 2(b)), however, a peak was detected only for the sample from pyridine, while the samples from acrylonitrile and julolidine show no peaks. On the basis of these results, N-doped graphene was synthesized from pyridine, and non-doped graphene was obtained from acrylonitrile and julolidine. C 1s peak of the sample from melamine appears at higher binding energy, which cannot be assigned to graphene. The intensity ratio of C 1s and N 1s for the sample from melamine exhibits the sample contains more nitrogen than carbon. From this result, graphene cannot be formed from melamine by depositing it onto a heated Pt(111) surface.

It is obvious that the final product using this method strongly depends on the starting materials. This dependence can arise from the strength of chemical bonds in source molecules. The bond strength of skeletal bonds in a pyridine molecule is similar to each other. Therefore nitrogen atoms can be incorporated into graphene when carbon atoms construct sp^2 network on a Pt surface kept at an appropriate heating temperature (Fig. 3(a)). In contrast, the single bonds in an acrylonitrile and a julolidine molecule are much more likely to be broken than the other skeletal bonds due to the weaker bond strength. Schematic illustration of growth model for acrylonitrile is shown in Fig. 3(b). Nitrogen atoms are separated off from carbon atoms and evaporate as volatile molecules such as HCN and C_2N_2.

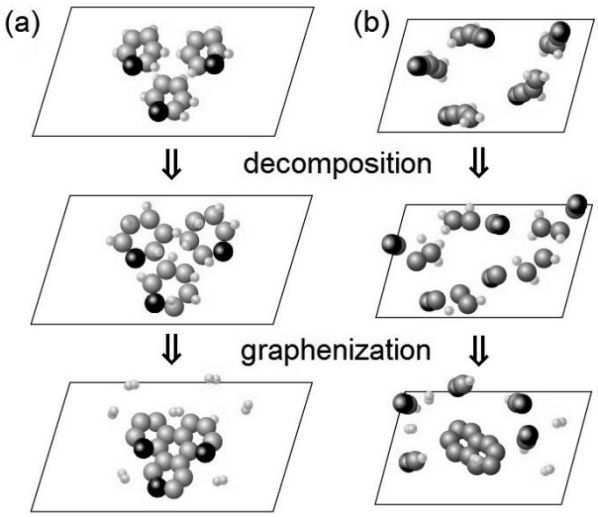

Fig. 3 Growth model of graphene on a heated Pt surface from (a) pyridine and (b) acrylonitrile.

2.2 Oxygen adsorption activity of N-doped graphene

Oxygen reduction reaction (ORR) activity is one of the most interesting topics of N-doped graphene. To elucidate the first step of the reaction, adsorption structure of oxygen on N-doped graphene was investigated by means of XPS. N-doped graphene synthesized from pyridine on a Pt(111) surface was exposed to 1.0×10^5 Pa oxygen for 10 min. Non-doped graphene from benzene was also exposed to oxygen.

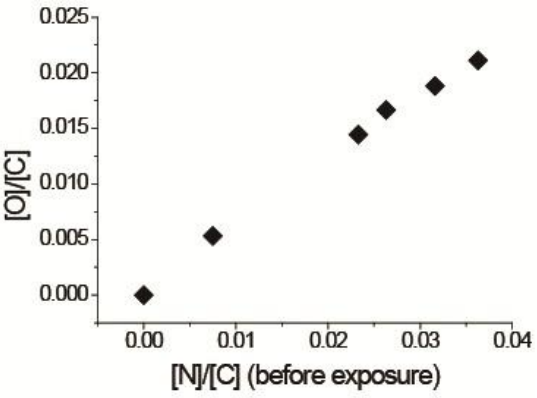

Fig. 4 Amount of adsorbed oxygen as a function of nitrogen content in N-doped graphene.

No O 1s peak was detected for non-doped graphene. On the other hand, N-doped graphene exhibits O 1s peaks which can be assigned to oxygen functional groups. The relationship between N content in N-doped graphene and the amount of adsorbed oxygen is shown in Fig. 4. The higher the N content of N-doped graphene is, the more oxygen atoms are adsorbed. It is expected the nitrogen atoms incorporated in graphene modify the electronic structure of adjacent atoms, and those atoms can be active sites for oxygen adsorption. I also observed the changes in N 1s peak shape after oxygen adsorption. The peak can be fitted with two Gaussian functions of which the center peaks locate at graphitic N (N atoms bonded with three sp^2 C neighbors) and pyridinic N (N atoms with two sp^2 C neighbors, refer to Fig.5). The total amount of nitrogen does not change after the exposure to oxygen, while the intensity ratio of graphitic N to pyridinic N changes.

Based on the results, N atoms incorporated in graphene enhance the oxygen adsorption. Oxygen chemically adsorbs onto N-doped graphene and cause structural change around N atoms.

2.3 Synthesis of B, N-Doped Graphene

In addition to N-doped graphene, I synthesized B, N-doped graphene in a same way by using hexaphenylborazine (HPB, $C_{36}H_{30}B_3N_3$, shown in Fig.1(e)) as a source material. HPB was deposited onto a Pt(111) surface heated at various temperatures and *in situ* XPS measurements were taken. The C 1s spectra of the samples show a peak shifts to lower binding energy down to 284.0 eV with increasing substrate temperature (T_S). N 1s peak becomes weaker as T_S increases. N 1s peak can be observed up to 600 °C, and disappears at 800 °C. In the region of B 1s, B 1s peak can be detected as high as T_S = 400 °C. Judged from these XPS data, HPB was decomposed on a heated Pt(111) surface and form graphene. Both boron and nitrogen doped graphene was synthesized at T_S = 400 °C and N-doped graphene grew at T_S = 600 °C, while non-doped graphene was obtained at T_S = 800 °C.

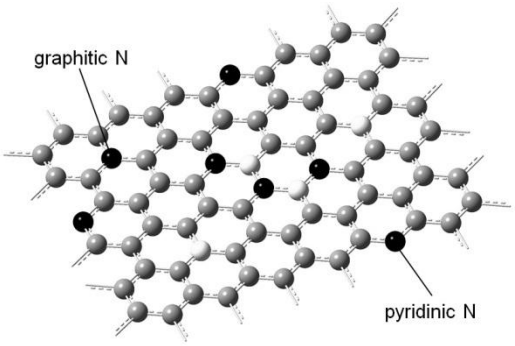

Fig. 5 Schematic illustration of B,N-doped graphene. Gray, black and white balls represent carbon, nitrogen and boron atoms, respectively.

3. Defect Formation on Graphene by Ultraviolet-Irradiation

The effect of UV-irradiation to graphene is investigated. Graphene was grown on several substrate, copper foil, Ru(0001) and Pt(111). Graphene on a Si wafer was also prepared by transferring graphene grown on Cu foil. I also used Highly Oriented Pyrolytic Graphite (HOPG) for comparison. Deuterium lamp was used as a UV-light source. Samples were UV-irradiated in various ambient at 10 Pa for 2 hours, followed by Raman spectroscopy.

Figure 6(a) shows the intensity ratios of the Raman D peak to the G peak (I_D/I_G). Graphene on a Si wafer (tGr) shows even higher I_D/I_G ratio, which indicates high density of defects, than graphene on other substrates. This result implies the suppression of defect formation by the interaction between graphene and substrates, because the Si surface hardly affects the electronic structure of graphene. The dotted line area in Fig. 6(a) is magnified in Fig. 6(b). The I_D/I_G ratio becomes higher for all irradiated samples except the one on a Pt(111) surface. The similar behavior in I_D/I_G ratio for graphene on a Ru(0001) surface and HOPG comes from the number of layers because multilayer graphene grows on a Ru(0001) surface while graphene on a Cu foil and a Pt(111) surface is a single layer. HOPG consists of a number of graphene layers, and hence exhibits a similar response to UV-irradiation. The difference in behavior between the graphenes on a Pt(111) surface and on Cu foil might be due to the Fermi level shift caused by metal contacts. The Fermi level of graphene shifts lower on a Pt surface, while contact with a Cu surface heightens the Fermi level. This opposite Fermi level shift affects the response of graphene to UV-light, and gives rise to different defect formation. It is clearly seen that samples irradiated in NH_3 have higher I_D/I_G ratio. Photon energy of Deuterium lamp is enough high for photodissociation reaction of NH_3 ($NH_3 \rightarrow NH_2 + H$), which generates active radicals. Therefore such radicals attack graphene and cause high I_D/I_G ratio.

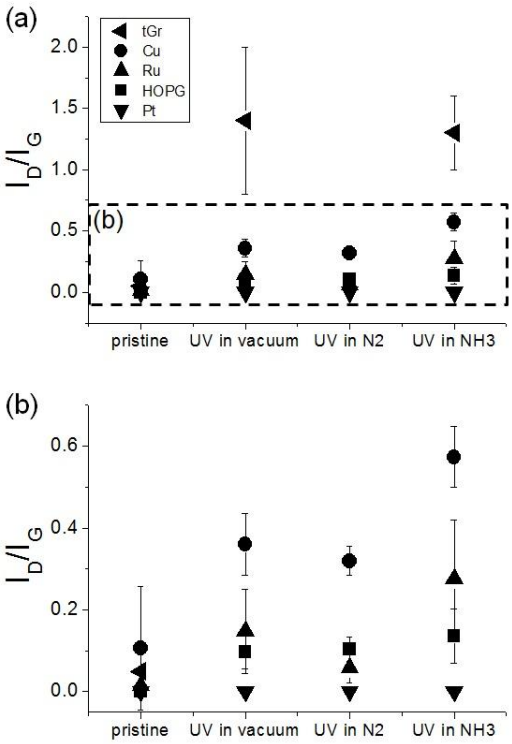

Fig. 6 (a) Intensity ratios of the Raman D peak to G peak. (b) The magnified figure of dotted line area in (a).

4. Summary

In my study, I developed methods of chemically doping graphene with heteroatoms and explore the defect formation of graphene by UV-irradiation. Several heteroatom-containing molecules were used in order to synthesize doped graphene on a Pt(111) surface by CVD process. I have clarified the relationship between the molecular structure and the potentiality of synthesizing doped graphene. Adsorption structure of oxygen on N-doped graphene was investigated with XPS. It was revealed that doped N atoms enhance the adsorption activity for oxygen, and structure of N-doped graphene changes by oxygen adsorption. Defect formation of graphene by UV-irradiation was also explored on several substrates and in several ambient. It became clear that defect formation is highly affected by substrates, and NH_3 ambient causes high I_D/I_G ratio as NH_3 produces active radicals through photodissociation reaction.